One stop shop: Flortaucipir PET differentiates amyloid positive and negative forms of neurodegenerative diseases

Jochen Hammes, MD^{1,2}, Gérard N Bischof, PhD ^{1,3}, Karl P Bohn, MD^{1,4}, Özgür Onur, MD^{5,6}, Anja Schneider, MD^{7,8}, Klaus Fliessbach, MD^{7,8}, Merle C Hönig, PhD^{1,9}, Frank Jessen, MD^{7,10,11}, Bernd Neumaier, PhD^{12,13}, Alexander Drzezga, MD^{1,7,9}, Thilo van Eimeren, MD^{1,5,7}

- 1) University of Cologne, University Hospital and Medical Faculty, Department of Nuclear Medicine, Multimodal Neuroimaging , Cologne, Germany
- 2) Radiologische Allianz, Hamburg, Germany
- 3) University of Cologne, Faculty of Mathematics and Natural Sciences, Cologne, Germany.
- 4) University of Bern, Inselspital University Hospital, Department of Nuclear Medicine, Bern, Switzerland
- 5) University of Cologne, University Hospital and Medical Faculty, Department of Neurology, Cologne, Germany.
- 6) Research Center Jülich, Molecular Organization of the Brain, Institute of Neuroscience and Medicine (INM-3), Jülich, Germany.
- 7) German Center for Neurodegenerative Diseases (DZNE), Bonn/Cologne, Germany.
- 8) University of Bonn, University Hospital Bonn, Department of Neurodegenerative Diseases and Geriatric Psychiatry, Bonn, Germany.
- 9) Research Center Jülich, Molecular Organization of the Brain, Institute of Neuroscience and Medicine (INM-2), Jülich, Germany.
- 10) University of Cologne, University Hospital and Medical Faculty, Department of Psychiatry, Cologne, Germany.
- 11) University of Cologne, University Hospital and Medical Faculty, Excellence Cluster on Cellular Stress Responses in Aging-Associated Diseases (CECAD) , Cologne, Germany
- 12) Research Center Jülich, Nuclear Chemistry, Institute of Neuroscience and Medicine (INM-5), Jülich, Germany.
- 13) University of Cologne, University Hospital and Medical Faculty, Institute of Radiochemistry and Experimental Molecular Imaging, Cologne, Germany.

Corresponding author:

Jochen Hammes, MD Multimodal Neuroimaging Group University Hospital Cologne, Kerpener Str. 62, 50937 Cologne, Germany Tel. +49 221 478-7570

Fax. +49 221 478-82845

Email: jochen.hammes@uk-koeln.de

Running title: Flortaucipir PET predicts amyloid status

Keywords: Flortaucipir, AV-1451, T807, Tau-PET, SSM/PCA

Word count abstract: 247

Word count manuscript body: 3104

ABSTRACT

Tau protein aggregations are a hallmark of pathology in the amyloid-associated Alzheimer's disease and some forms of non-amyloid-associated fronto-temporal lobar degeneration (FTLD). In recent years, several tracers for in-vivo tau imaging are under evaluation. This study investigates the ability of Flortaucipir PET to not only assess tau-positivity but in addition also to differentiate between amyloid-positive and -negative forms of neurodegeneration based on different Flortaucipir PET signatures.

Methods

Flortaucipir PET data of 35 patients with amyloid-positive, 19 patients with amyloid-negative forms of neurodegeneration and 17 healthy controls were included in a data-driven scaled subprofile modelling/principal component analysis (SSM/PCA) identifying spatial covariance patterns. SSM/PCA component pattern expression strengths (PES) were tested for their ability to predict amyloid status in a receiver operating characteristic analysis and validated with a leave-one-out approach.

Results

PES predicted amyloid status with a sensitivity of 0.94 and a specificity of 0.83. A support vector machine classification based on PES in two different SSM/PCA components yielded a prediction accuracy of 98%. Anatomically, prediction performance was driven by parietooccipital grey matter in amyloid-positive patients vs. predominant white matter binding in amyloid-negative neurodegeneration.

Conclusion

SSM/PCA derived binding patterns of Flortaucipir differentiate between amyloid positive and negative neurodegenerative diseases with high accuracy. Flortaucipir PET alone may convey additional information equivalent to an amyloid PET. Together with a perfusion-weighted early-phase acquisition (FDG-PET equivalent), a single scan potentially contains comprehensive

information on amyloid (A), tau (T) and neurodegeneration (N) status as required by recent biomarker classification algorithms (A/T/N).

INTRODUCTION

Aggregation of specific proteins are a hallmark of pathology in the two of the most common forms of neurodegenerative dementia, Alzheimer's disease (AD) and fronto-temporal lobar degeneration (FTLD). It is assumed that in AD, abundant extracellular ß-amyloid plaques are present in the brain many years before symptomatic disease onset, whereas spreading of intracellular neurofibrillary tau tangles across the cortex appears to be more closely associated with neuronal injury and, thus, clinical symptoms(1,2). The advent of amyloid and tau PET tracers has therefore been a major breakthrough for accurate and early diagnosis of AD. In FTLD, on the other hand, amyloid pathology is typically absent, while the majority of cases are tau-positive and most tau-negative forms are related to TDP protein pathology(3).

However, ultrastructurally, tau protein aggregations are not uniform across disease entities. In short, in amyloid-associated pathology tau protein aggregates occur in the variant of paired helical filaments (PHF) while in the non-amyloid associated diseases, mainly straight filaments (SF) are present(4,5).

Recently, Flortaucipir and other tau PET tracers demonstrated great potential to identify tau pathology in the living human brain(6,7). Flortaucipir had originally been developed as a tracer for pathology in tau AD (PHF-tau) generally showing a strong binding in affected cortical areas(6,7). Flortaucipir also seems to be sensitive for non-AD tau pathology (SF-tau). In the behavioral variant of frontotemporal dementia (bvFTD), a disease mostly associated with SF-tau, Flortaucipir shows increased binding in the cortex and subcortical white and gray matter(8). Complementing these findings, a binding also been demonstrated in familial cases with confirmed mutations of the microtubule-associated protein tau (MAPT) gene(9,10). Moreover, a recent study has shown increased Flortaucipir binding in the non-fluent variant of primary progressive aphasia(11), a syndrome caused by non-amyloid related tau protein pathology in about 50 % of the cases(12).

Interestingly, there is also evidence, that Flortaucipir has a similar affinity to TDP-43-pathology as patients with semantic variant of primary progressive aphasia (mostly caused by TDP-43 pathology) exhibit elevated Flortaucipir binding in affected brain areas. The binding

intensities in non-amyloid associated neurodegenerative diseases seem generally lower than in AD variants(13–15).

Regardless of binding specificity to a certain type of protein pathology, Flortaucipir PET might still be helpful for biomarker classification according to the A/T/N system(16). Based on the aforementioned data, we expect high cortical Flortaucipir-binding in amyloid-positive (A+T+N+) cases, elevated Flortaucipir binding in cortical and subcortical gray and white matter in amyloid-negative forms of neurodegeneration (A-(T+)N+) and no elevated binding in healthy subjects (T-status in brackets, since Flortaucipir binding does not sufficiently differentiate between the presence of tau and TDP-43 pathology). This study investigates the ability of Flortaucipir PET to predict amyloid status in typical and atypical AD as well as behavioral and language variants of FTLD-type neurodegenerative diseases with a conventional voxel-wise mass univariate approach, a data-driven principal component analysis based approach and by applying a support vector machine based supervised learning model.

MATERIAL AND METHODS

The protocol for the study has received prior approval by the appropriate Institutional Review Board. Informed consent was obtained from each subject.

54 patients were clinically diagnosed with typical or atypical AD (i.e. logopenic variant of primary progressive aphasia or behavioral variant of AD) or a variant of FTLD at the interdisciplinary center for memory disorders of the University Hospital Cologne and the Department of Psychiatry, University Hospital Bonn. Diagnosis was supported by the diagnostic FDG and amyloid PET imaging results as well as results of cerebrospinal fluid (CSF) analysis measuring amyloid and tau protein concentration. Amyloid and Flortaucipir PET scans were unanimously visually classified as positive or negative by three experienced raters (AD, TvE, JH). In 13 cases (FTLD 7, AD 4, atypical AD 2), only CSF amyloid information but no amyloid PET data was available. Cutoff-value for amyloid-positivity was a CSF amyloid-beta 1-42 concentration of 650 pg/ml. Patient characteristics are listed in table 1.

Patients underwent ¹⁸F-Flortaucipir (n = 54) and ¹⁸F-FDG PET (n= 51) imaging. All scans were performed at the Department of Nuclear Medicine, University Hospital Cologne, Germany, with a Siemens Biograph mCT Flow 128 Edge scanner (Siemens, Knoxville, TN). A low dose computed tomography scan was performed for attenuation correction (ACCT) prior to the PET acquisition. All PET scans were iteratively reconstructed using a 3-D OSEM algorithm (four iterations, 12 subsets, Gaussian filter: 5 mm Full width at half maximum, 400 × 400 matrix, slice thickness of 3 mm). For FDG PET, a ten minute acquisition was performed 30 minutes after injection of 200 MBq ¹⁸F-FDG. Flortaucipir PET was acquired for 15 minutes, 90 minutes after injection of 250 MBq of ¹⁸F-Flortaucipir.

All scans were processed using Statistical Parametric Mapping (SPM) version 12 (Wellcome Trust Centre for Neuroimaging, Institute of Neurology, University College London). PET images were in register with their corresponding ACCT, which was spatially normalized to the Neuro Imaging Tools & Resources Collaboratory CT-template (https://www.nitrc.org/projects/clinicaltbx/). Normalization parameters were subsequently

applied to the PET-images. All calculations were performed in the template derived MNI-152 anatomical space. Standard uptake value ratio (SUVR) images were calculated employing inhouse scripts in MATLAB R2016a (The MathWorks, Inc, Natick, MA, USA) using the cerebellar grey matter of the Hammersmith n30r83 atlas (17) as reference region. MRI scans have been performed in the routine clinical workup of the dementia syndromes and major vascular components were excluded before the patients were referred to the nuclear medicine department for PET imaging. However, these scans were not acquired according to a standardized acquisition protocol and could therefore not been used for image preprocessing.

Flortaucipir binding in most affected regions

All regions of the atlas were divided in a white (WM) and grey matter (GM) portion by voxel-wise multiplication with SPM binarized tissue probability maps (threshold 0.50) and then employed in volume of interest (VOI) analysis. For each subject and atlas region, average FDG and Flortaucipir SUVR were extracted separately for WM and GM. For each subject the GM atlas region that was most affected by neurodegeneration was identified via search for the individually lowest SUVR in FDG PET. Individual regions of highest cortical Flortaucipir SUVR were identified analogously. GM and WM SUVRs as well as GM-WM-SUVR-ratios were compared between the A+T+N+ and the A-(T+)N+ group with two-sample t-tests.

Whole-brain comparisons

A voxel wise t-test comparing Flortaucipir SUVR images of the A+T+N+ and the A-(T+)N+ group was performed in SPM. FWE corrected p-values < 0.05 were considered significant. Groupwise t-tests comparing average tracer binding of both groups against a previously established set of 17 healthy controls (HC) (2,18,19) and comparing binding between A+T+N+ and A-(T+)N+ patients were performed.

Classification using data-driven patterns

As a data-driven approach, scaled subprofile model of principal component analysis (SSM-PCA) was implemented. This method was initially developed to identify disease-specific cerebral metabolic covariance patterns in FDG PET (20). Measuring the individual expression strength of

disease related patters has proven very helpful in the early diagnosis of several neurodegenerative disorders (21). We performed a similar approach on all 71 Flortaucipir scans to identify covariance patterns possibly capable of group differentiation. Components derived from Flortaucipir SSM-PCA explaining at least 10% of variance in the dataset were tested for their ability to predict amyloid-status by measuring individual pattern expression. Pattern expression scores were calculated as scalar products of PET image matrices and PCA components similar to our previous work (22). A receiver operating characteristic (ROC) analysis was performed to identify an optimal threshold of pattern expression score with optimal sensitivity and specificity. Areas under the ROC curves (AUC) were calculated as measurement of prediction accuracy. ROC and AUC analyses were cross-validated with a leave-one-out approach.

In a second step, SSM/PCA was performed separately in subgroups consisting of either only A+T+N+ patients and healthy controls or only A-(T+)N+ patients and controls to identify the most dominant patterns characterizing areas of highest variance in the respective subgroup. For these two patterns expression scores were calculated for each subject. PCA patterns explaining >10% of variance were included in the subsequent analyses. A support vector machine model for prediction of amyloid status based on the 2-dimensional pattern expression scores was set up. Amyloid status prediction accuracy of pairs of PCA patterns was determined and validated in a leave-one-out approach.

RESULTS

Flortaucipir PET scans of both the A+T+N+ and A-(T+)N+ group were visually rated as containing increased regional binding relative to background level. Representative cases (Fig. 1) with elevated Flortaucipir binding of both groups as well as a scan of a healthy control subject are shown in Figure 1A. Voxel-wise comparisons of average tracer binding in the A-(T+)N+ and the A+T+N+ patients against healthy controls are depicted in Figure 1B and 1C. A+T+N+ patients showed a typical AD pattern with a predominant Flortaucipir binding in the posterior cingulate, the parieto-temporal and the frontal cortex. In the A-(T+)N+ group, the comparison to healthy controls revealed an elevated average binding in the cerebral white matter most prominently in frontal and temporal regions.

The voxel wise t-test comparing A+T+N+ to A-(T+)N+ patients revealed a higher average Flortaucipir binding in the precuneus, the parieto-temporal and frontal cortices in A+T+N+ cases, while in the A-(T+)N+ patients, average tracer binding was higher in the cerebral white matter in the semi oval center, the pallidum and the substantia nigra (T-maps are depicted in Figure 1D, detailed voxel-wise T-test-results and coordinates can be found in the supplementary material in the form of SPM output graphics, i.e. Supplemental Figures 1 and 2).

Regional SUVRs and GM to WM ratios in regions most strongly affected by pathology as defined by either lowest FDG metabolism or highest Flortaucipir binding are depicted in Fig. 2. GM Flortaucipir uptake in regions with decreased FDG metabolism is significantly higher in A+T+N+ than in A-(T+)N+ patients (Figure 2C, p = 0.002). This group differentiation is even stronger for GM to WM ratios of areas with decreased FDG metabolism (Fig. 3D, p < 0.001) indicating relatively high WM uptake in these regions.

A combination of the first four components derived from SSM/PCA explained more than 50 % (1st component 29.5 %, 2nd component 10.1 %, 3rd component 7.7 and 4th component 5.3) of the variance in the full set comprising 71 Flortaucipir PET scans. Component one mainly consists of positive values in the cerebral white matter and negative values predominantly in cortical areas

that are typically affected in AD, i.e. precuneus, parieto-temporal cortex and fronto-lateral cortex (Figure 3A).

The expression of component one was able to predict amyloid status with a sensitivity of 0.94 and a specificity of 0.83, (AUC = 0.95, See Figure 3C for ROC curve), while the expression of the second PCA pattern predicted amyloid status with a sensitivity of 0.46, a specificity of 0.95 with an AUC of 0.64. Amyloid status prediction with components of higher orders resulted in lower values for sensitivity, specificity and AUC. A Leave-one-out cross validation with pattern expression scores of the first PCA pattern yielded a sensitivity of 0.78 and specificity of 0.84 with an AUC of 0.81 for amyloid status prediction.

The 2-dimensional approach (Fig. 4) generated separate sets of patterns in 1) a subgroup SSM/PCA of only A+T+N+ patients and HC and 2) a subgroup SSM/PCA of A-(T+)N+ patients and HC. A GM-dominant pattern in the first A+T+N+/HC subgroup analysis explained 27 % of total variance in the dataset and was selected as pattern of first dimension. A WM-dominant pattern derived from the A-(T+)N+/HC subgroup explained 12% of variance and was selected as pattern of second dimension. The selected PCA patterns are depicted in Figure 4B, the 2-dimensional pattern expression scores (square root transformed for better visibility) are shown in Figure 4B. Amyloid status prediction based on 2-dimensional pattern expression yielded an accuracy of 98.5%. The leave-one-out cross validation resulted in a minor reduction of prediction accuracy to 94.0%.

DISCUSSION

Here, we demonstrate for the first time that Flortaucipir PET can not only detect taurelated pathology, but can also be used to infer the probable amyloid status by analyzing Flortaucipir PET signal intensity and distribution across white and grey matter. Specifically, we could distinguish with high accuracy between amyloid positive and negative cases in a mixed group of typical and atypical AD as well as behavioral and language variants of FTLD-type neurodegenerative diseases.

According to first available studies, tau-PET may be less sensitive than amyloid-PET in the early diagnosis of Alzheimer's disease (23), however, typical and atypical AD cases show a distinct Flortaucipir binding pattern that clearly separates patients from healthy controls (2,18,24). The Flortaucipir binding in bvFTD patients is distinct from the AD pattern and seems to be predominantly expressed in subcortical WM and GM and generally lower in signal intensity (13,14,8). The presence of tau pathology in both WM and GM in patients with bvFTLD has been confirmed in histopathological studies (5,25). While there is evidence of a correlation between ante-mortem Flortaucipir-PET imaging and post-mortem histopathological findings in three AD patients (26), data on other diseases such as bvFTLD is limited. A combined immunohistochemical and autoradiographic study analyzing post-mortem samples of patients with AD and non-AD tauopathies found only limited sensitivity to tau protein aggregations in early disease stages, and a high variability in Flortaucipir binding between and within cases (27). Recently, Marquié et al. reported no post mortem binding of [3H]Flortaucipir in autoradiography in cases of histophathologically confirmed cases of non-AD tauopathies, including a case of MAPT P301L mutation leading to frontotemporal dementia (28). However, artifacts caused during the process of tissue fixation and deparaffinization might be responsible for this discrepancy between in vivo and in vitro findings.

Histopathologically, tau pathology occurs predominantly in the cortex in AD (29) while in FTLD variants, a severe white matter tau burden is present (30,31). This difference might account for the fundamentally different binding behavior in amyloid positive and amyloid negative patients regarding subcortical regions. To date, it remains unclear whether the Flortaucipir

binding in FTLD is due to a specific affinity of the tracer to isoforms of tau protein aggregates as they occur in these diseases or due to an unspecific affinity to any kind of co-pathology occurring simultaneously and in similar regions. However, the lower Flortaucipir SUVRs in the cortex in comparison to subcortical regions in A-(T+)N+ patients might be suggestive of a not directly tau protein-related binding target that more dominantly occurs in white matter together with cortical and subcortical tau pathology as it can be present in amyloid negative forms of neurodegeneration.

There is increasing evidence that Flortaucipir also has a binding affinity to monoamine oxidases (MAO) isoforms confirmed by enzyme inhibition assays, autoradiography and in vivo PET (32–34). A recent in vitro study showed a comparable binding strength of Flortaucipir to tau fibrils and MAO (35). However, Hansen et al. described that Flortaucipir PET signal cannot be decreased by administration of MAO-inhibitors (36). In comparison to THK5351, another ligand initially developed to specifically bind to tau protein accumulations in AD, Flortaucipir's off target binding caused by MAO isoforms appears relatively lower (37,38).

Value of Flortaucipir PET

In this study we show that it may be possible with Flortaucipir PET to discriminate amyloid positive from amyloid negative forms of neurodegeneration. This distinction can be performed by evaluating the expression strength of the distinctive pattern derived from SSM/PCA according to the concept of disease specific patterns as first described by the Eidelberg group (20). Given the data suggesting that Flortaucipir may not only bind to tau protein aggregations but potentially also to TDP-43 protein pathology, a definite proof of presence of tau pathology cannot be derived from a Flortaucipir scan. Thus, the accuracy of predicting the amyloid status with the SSM/PCA based 2D pattern expression score was not necessarily achieved by Flortaucipir binding to specific molecular targets, but rather distinct patterns of a mixture of on-target and off-target binding that are characteristic for different neurodegenerative conditions which themselves are associated with different degree of amyloid depositions.

In the context of molecular therapy strategies specifically targeting protein aggregations, the data presented in this study may not be sufficient to decide on the suitability of patients for specific therapy trials. First of all, that is the case for tau protein aggregations whose presence cannot definitely be determined by Flortaucipir PET in non-AD tauopathies due to possible off-target binding. Secondly, even though we have shown that 2D-pattern expression scores work well in discriminating Flortaucipir distribution patterns of diseases that are associated with different degrees of amyloid pathology, based on only the data presented in this study, a generalization to predict quantitative amyloid biomarkers solely based on Flortaucipir distribution patterns is not possible

However, Flortaucipir can still be of great value in the diagnosis of neurodegeneration:

- 1. According to the present literature, a quantification of tau pathology in amyloid positive forms of neurodegeneration is possible with Flortaucipir PET (*39,40*).
- 2. Our group has shown before that early acquisition phases with Flortaucipir provide equivalent information on neuronal integrity as an additional FDG-PET (41). In addition to that combined early and late acquisition windows might be more sensitive in early phases of amyloid positive neurodegeneration (42).
- 3. The results from this study suggest that additional non-quantitative information about the probable amyloid status can be derived without an additional amyloid PET examination as shown in this study.

These findings together provide the opportunity for a one-stop-shop diagnostic approach where a single Flortaucipir PET scan with a combined early and late acquisition phase might render both additional FDG and amyloid PET scans redundant. Consequently, such a single tracer scan procedure may possibly provide comprehensive information on probable amyloid status (A), tau positivity (T) and level of neurodegeneration (N) as required by recent biomarker classification algorithms (A/T/N).

Limitations

Although the distinctive pattern that we have established in this study seems to be able to distinguish amyloid positive from amyloid negative patients with neurodegenerative diseases, it does not allow for a final diagnosis of a specific neurodegenerative disease (e.g. bvFTLD or FTLD variants primarily affecting language). This is due to the small sample size and the heterogeneous composition of the group of amyloid negative patients. Because of the rather low prevalence of those diseases and the retrospective nature of this study, we had to compose this group from a set of patients with different neurodegenerative diseases all sharing amyloid negativity as determined mostly by amyloid PET (7 of 19 amyloid negative cases only had CSF information available) as common denominator. Especially in the amyloid negative group, diagnoses are mostly only based on clinical impression, PET findings and CSF status and lack a definitive confirmation of pathology. This might have introduced a certain diagnostic bias into the study. For example, it cannot be ruled out entirely that cases in early stages of atypical AD with still normal CSF amyloid levels, no amyloid PET data available and a non-AD-characteristic hypometabolism pattern FDG-PET have been misclassified.

Even though there was no significant age difference between A+T+N+ and A-(T+)N+ patients, a potential influence of age on the binding pattern of Flortaucipir cannot be ruled out entirely.

SUVR-calculation to an average activity concentration in a reference region always bears the risk of causing normalization artifacts. To date, no standard reference region has been established for Flortaucipir across various disease entities. To minimize artifacts due to elevated Flortaucipir binding subcortical nuclei of the cerebellum as it has been described in amyloid negative forms of neurodegeneration, we have decided to pick the cerebellar gray matter as a reference region for SUVR-calculation. However, the SSM/PCA procedure contains a normalization routine in itself that uses all included brain voxels as intensity reference. The basically comparable distinction-patterns derived from both the SSM/PCA approach and the classical voxel-wise SPM based approach suggest that normalization artifacts did not strongly affect our data.

In 13 cases, no amyloid PET was available and information on amyloid status could only be obtained from CSF analyses. Although there is a very high concordance between PET and CSF-derived amyloid status, especially in amyloid-positive cases, a small number of inaccurate group assignments (A+ vs. A-) cannot be ruled out entirely.

Lastly, this study only included symptomatic patients. Therefore, based on the results of this study no statement can be made, whether a prediction of amyloid status with Flortaucipir PET might be possible for presymptomatic or very early stages of neurodegenerative diseases.

CONCLUSION

We have shown that Flortaucipir PET is able to differentiate between amyloid positive and amyloid negative forms of neurodegeneration, possibly eliminating the need of an additional amyloid PET scan or a cerebrospinal fluid examination. When performed as dual phase scan with an additional early perfusion-weighted acquisition window replacing an additional FDG PET scan, Flortaucipir PET holds the potential to significantly reduce radiation exposure and the complexity of the diagnostic workup in patients with suspected neurodegenerative diseases, allowing to provide comprehensive A/T/N-classification information in a single examination.

ACKNOWLEDGEMENTS

This study was supported by the Deutsche Forschungsgemeinschaft (DFG) by grant DR 445/9-1

Disclosure

AD: Research support and speaker honoraria by AVID/Lilly Radiopharmaceuticals, which owns patent rights to Flortaucipir and Siemens Healthineers.

TvE: lecture and consulting honoraria from AVID/Lilly Radiopharmaceuticals, which owns patent rights to Flortaucipir.

All other authors report no conflict of interest.

Key Points

QUESTION: Is prediction of amyloid status of patients with neurodegenerative diseases possible with Flortaucipir PET?

PERTINENT FINDINGS: Binding patterns of Flortaucipir predict amyloid status in neurodegenerative diseases with high accuracy. Flortaucipir PET alone may convey additional information equivalent to an amyloid PET.

IMPLICATIONS FOR PATIENT CARE: To derive information on amyloid status from Flortaucipir PET possibly eliminates the need of an additional amyloid PET scan or a cerebrospinal fluid examination.

REFERENCES

- 1. Jack CR, Wiste HJ, Schwarz CG, et al. Longitudinal tau PET in ageing and Alzheimer's disease. *Brain*. 2018;141:1517-1528.
- 2. Bischof GN, Jessen F, Fliessbach K, et al. Impact of tau and amyloid burden on glucose metabolism in Alzheimer's disease. *Ann Clin Transl Neurol*. 2016;3:934-939.
- 3. Mackenzie IRA, Neumann M, Bigio EH, et al. Nomenclature and nosology for neuropathologic subtypes of frontotemporal lobar degeneration: an update. *Acta Neuropathol (Berl)*. 2010;119:1-4.
- 4. Goedert M, Spillantini MG, Crowther RA. A brief history of tau. *Clin Chem.* 2015;61:1417-1418.
- 5. Kovacs GG. Invited review: Neuropathology of tauopathies: principles and practice. *Neuropathol Appl Neurobiol*. 2015;41:3-23.
- 6. Bischof GN, Endepols H, van Eimeren T, Drzezga A. Tau-imaging in neurodegeneration. *Methods San Diego Calif.* 2017;130:114-123.
- 7. Hammes J, Bischof GN, Drzezga A. Molecular imaging in early diagnosis, differential diagnosis and follow-up of patients with neurodegenerative diseases. *Clin Transl Imaging*. 2017;5:465–471.
- 8. Cho H, Seo SW, Choi JY, et al. Predominant subcortical accumulation of 18F-flortaucipir binding in behavioral variant frontotemporal dementia. *Neurobiol Aging*. 2018;66:112-121.
- 9. Smith R, Puschmann A, Schöll M, et al. 18F-AV-1451 tau PET imaging correlates strongly with tau neuropathology in MAPT mutation carriers. *Brain*. 2016;139:2372-2379.
- 10. Jones WRB, Cope TE, Passamonti L, et al. [18F]AV-1451 PET in behavioral variant frontotemporal dementia due to MAPT mutation. *Ann Clin Transl Neurol*. 2016;3:940-947.
- 11. Utianski RL, Whitwell JL, Schwarz CG, et al. Tau uptake in agrammatic primary progressive aphasia with and without apraxia of speech. *Eur J Neurol*. 2018;25:1352-1357
- 12. Bonner MF, Ash S, Grossman M. The new classification of primary progressive aphasia into semantic, logopenic, or nonfluent/agrammatic variants. *Curr Neurol Neurosci Rep.* 2010;10:484.
- 13. Tsai RM, Bejanin A, Lesman-Segev O, et al. 18F-flortaucipir (AV-1451) tau PET in frontotemporal dementia syndromes. *Alzheimers Res Ther*. 2019;11:13.
- 14. Smith R, Santillo AF, Waldö ML, et al. 18F-Flortaucipir in TDP-43 associated frontotemporal dementia. *Sci Rep.* 2019;9:6082
- 15. Makaretz SJ, Quimby M, Collins J, et al. Flortaucipir tau PET imaging in semantic variant primary progressive aphasia. *J Neurol Neurosurg Psychiatry*. 2018;89:1024-1031

- 16. Jack CR, Bennett DA, Blennow K, et al. A/T/N: An unbiased descriptive classification scheme for Alzheimer disease biomarkers. *Neurology*. 2016;87:539-547.
- 17. Hammers A, Allom R, Koepp MJ, et al. Three-dimensional maximum probability atlas of the human brain, with particular reference to the temporal lobe. *Hum Brain Mapp*. 2003;19:224-247.
- 18. Hoenig MC, Bischof GN, Seemiller J, et al. Networks of tau distribution in Alzheimer's disease. *Brain*. 2018;141:568-581.
- 19. Hammes J, Bischof GN, Giehl K, et al. Elevated in vivo [18F]-AV-1451 uptake in a patient with progressive supranuclear palsy. *Mov Disord*. 2017;32:170-171.
- 20. Eidelberg D. Metabolic brain networks in neurodegenerative disorders: a functional imaging approach. *Trends Neurosci.* 2009;32:548-557.
- 21. Mattis PJ, Niethammer M, Sako W, et al. Distinct brain networks underlie cognitive dysfunction in Parkinson and Alzheimer diseases. *Neurology*. 2016;87:1925-1933.
- 22. Granert O, Drzezga AE, Boecker H, et al. Metabolic topology of neurodegenerative disorders: influence of cognitive and motor deficits. *J Nucl Med.* 2015;56:1916-1921.
- 23. Johnson KA, Schultz A, Betensky RA, et al. Tau positron emission tomographic imaging in aging and early Alzheimer disease. *Ann Neurol*. 2016;79:110-119.
- 24. Dronse J, Fliessbach K, Bischof GN, et al. In vivo patterns of tau pathology, amyloid-β burden, and neuronal dysfunction in clinical variants of Alzheimer's disease. *J Alzheimers Dis*. October 2016:1-7.
- 25. Zhukareva V, Mann D, Pickering-Brown S, et al. Sporadic Pick's disease: A tauopathy characterized by a spectrum of pathological τ isoforms in gray and white matter. *Ann Neurol*. 2002;51:730-739.
- 26. Siderowf A, Keene C, Beach T, et al. Comparison of regional flortaucipir PET SUVr values to quantitative tau histology and quantitative tau immunoassay in patients with Alzheimer's disease pathology: a clinico-pathological study. *J Nucl Med*. 2017;58:629-629.
- 27. Wren MC, Lashley T, Årstad E, Sander K. Large inter- and intra-case variability of first generation tau PET ligand binding in neurodegenerative dementias. *Acta Neuropathol Commun.* 2018;6:34.
- 28. Marquié M, Normandin MD, Meltzer AC, et al. Pathological correlations of [F-18]-AV-1451 imaging in non-alzheimer tauopathies. *Ann Neurol*. 2017;81:117-128.
- 29. Nasrabady SE, Rizvi B, Goldman JE, Brickman AM. White matter changes in Alzheimer's disease: a focus on myelin and oligodendrocytes. *Acta Neuropathol Commun.* 2018;6:22.
- 30. Irwin DJ, Brettschneider J, McMillan CT, et al. Deep Clinical and Neuropathological Phenotyping of Pick's Disease. *Ann Neurol.* 2016;79:272-287.

- 31. Sakae N, Josephs KA, Litvan I, et al. Neuropathologic basis of frontotemporal dementia in progressive supranuclear palsy. *Mov Disord*. 2019 Nov;34:1655-1662.
- 32. Murugan NA, Chiotis K, Rodriguez-Vieitez E, Lemoine L, Ågren H, Nordberg A. Cross-interaction of tau PET tracers with monoamine oxidase B: evidence from in silico modelling and in vivo imaging. *Eur J Nucl Med Mol Imaging*. 2019;46:1369-1382.
- 33. Drake LR, Pham JM, Desmond TJ, et al. Identification of AV-1451 as a weak, nonselective inhibitor of monoamine oxidase. *ACS Chem Neurosci*. 2019;10:3839-3846.
- 34. Xia C-F, Arteaga J, Chen G, et al. [(18)F]T807, a novel tau positron emission tomography imaging agent for Alzheimer's disease. *Alzheimers Dement*. 2013;9:666-676.
- 35. Vermeiren C, Motte P, Viot D, et al. The tau positron-emission tomography tracer AV-1451 binds with similar affinities to tau fibrils and monoamine oxidases. *Mov Disord*. 2018;33:273-281.
- 36. Hansen AK, Brooks DJ, Borghammer P. MAO-B inhibitors do not block in vivo flortaucipir([18F]-AV-1451) binding. *Mol Imaging Biol. 2018 Jun; 20:356-360*.
- 37. Kim HJ, Cho H, Park S, et al. THK5351 and flortaucipir PET with pathological correlation in a Creutzfeldt-Jakob disease patient: a case report. *BMC Neurol*. 2019;19:211
- 38. Ng KP, Pascoal TA, Mathotaarachchi S, et al. Monoamine oxidase B inhibitor, selegiline, reduces 18F-THK5351 uptake in the human brain. *Alzheimers Res Ther*. 2017;9:25.
- 39. Smith R, Wibom M, Pawlik D, Englund E, Hansson O. Correlation of in vivo [18F]flortaucipir with postmortem Alzheimer disease tau pathology. *JAMA Neurol*. 2019;76:310-317.
- 40. Saint-Aubert L, Lemoine L, Chiotis K, Leuzy A, Rodriguez-Vieitez E, Nordberg A. Tau PET imaging: present and future directions. *Mol Neurodegener*. 2017;12:19.
- 41. Hammes J, Leuwer I, Bischof GN, Drzezga A, van Eimeren T. Multimodal correlation of dynamic [18F]-AV-1451 perfusion PET and neuronal hypometabolism in [18F]-FDG PET. *Eur J Nucl Med Mol Imaging*. 2017;44:2249-2256.
- 42. Eimeren T van, Bischof GN, Drzezga A. Is tau imaging more than just upside-down 18F-FDG imaging? *J Nucl Med*. 2017;58:1357-1359.

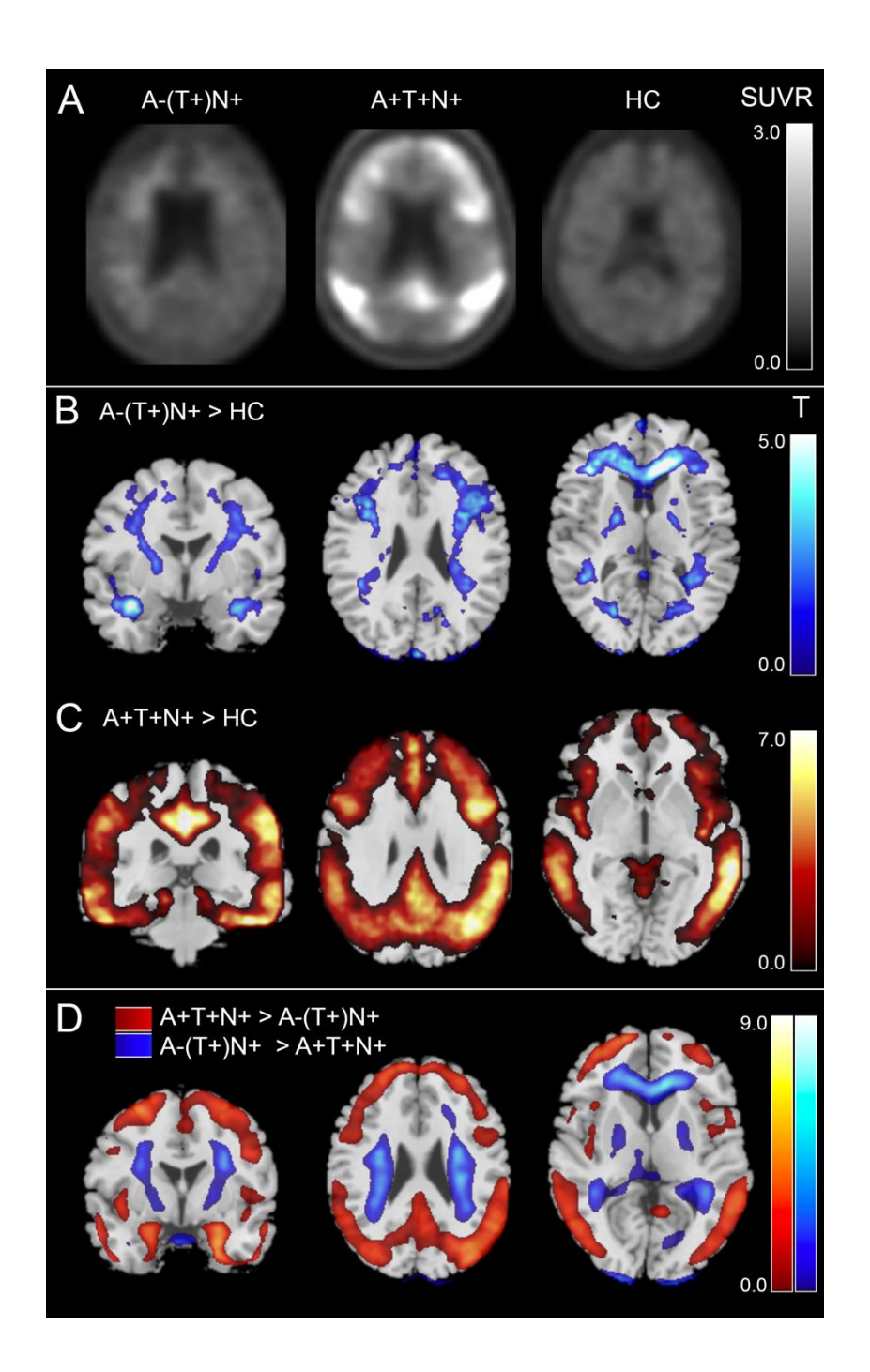


FIGURE 1: A) Flortaucipir binding in representative cases (A-(T+)N+, healthy controls). Displayed are SUVR values relative to the cerebellar gray. B, C) Results of group wise comparison of average Flortaucipir signal against healthy controls. (B: Amyloid negative group > healthy controls, C: Amyloid positive group > healthy controls). D) Results of between group comparison of average Flortaucipir signal in A+T+N+ vs. A-(T+)N+ patient (red: A+ > A-, blue A- > A+). T-values above 5.29 are statistically significant.

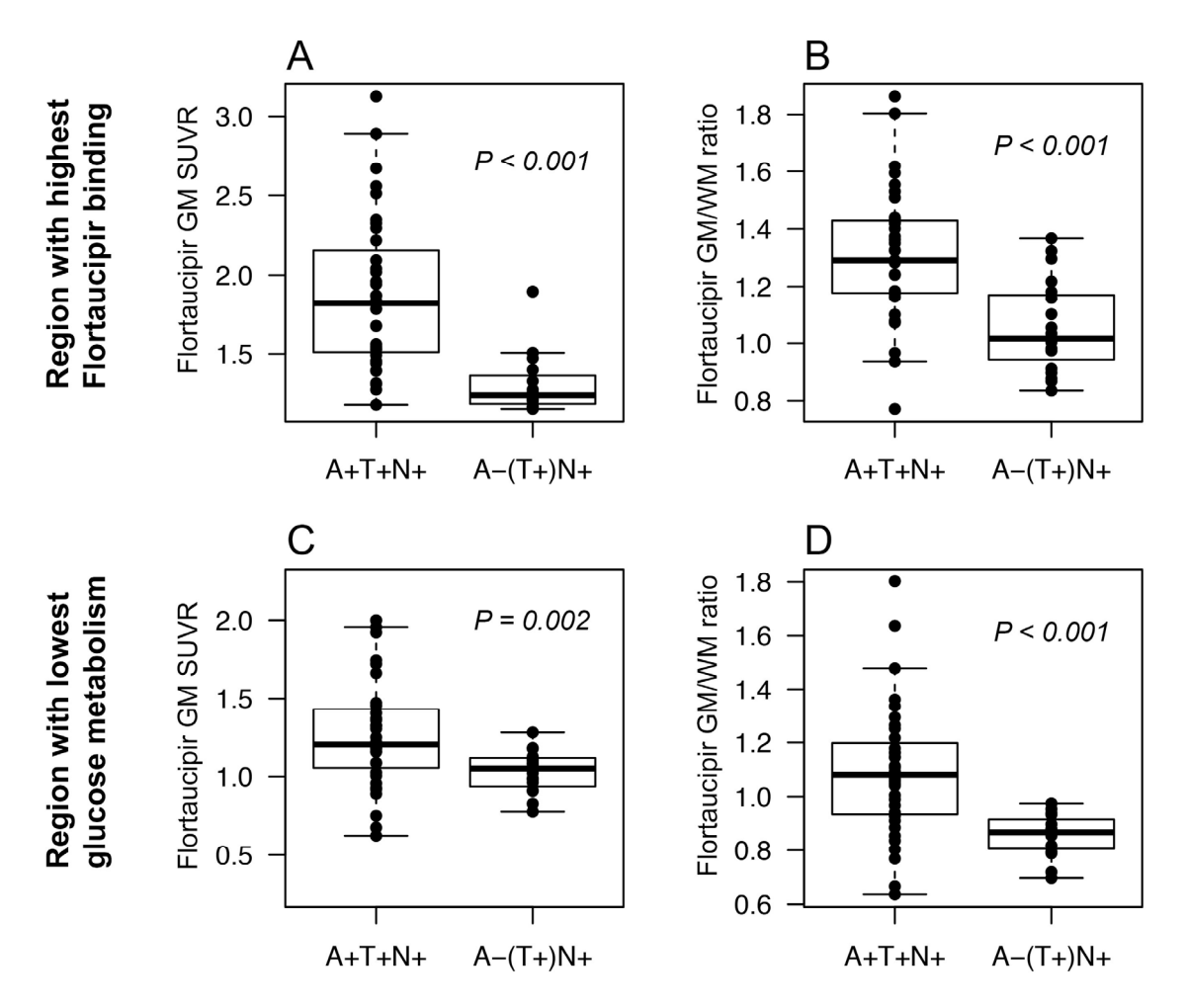


FIGURE 2: Flortaucipir binding in most affected regions A) Highest regional cortical GM Flortaucipir SUVR, B) GM/WM-ratio of Flortaucipir SUVR in atlas region with highest Flortaucipir signal, C) Cortical GM Flortaucipir SUVR in atlas region with lowest glucose metabolism, D) GM/WM-ratio of Flortaucipir SUVR in region with lowest glucose metabolism.

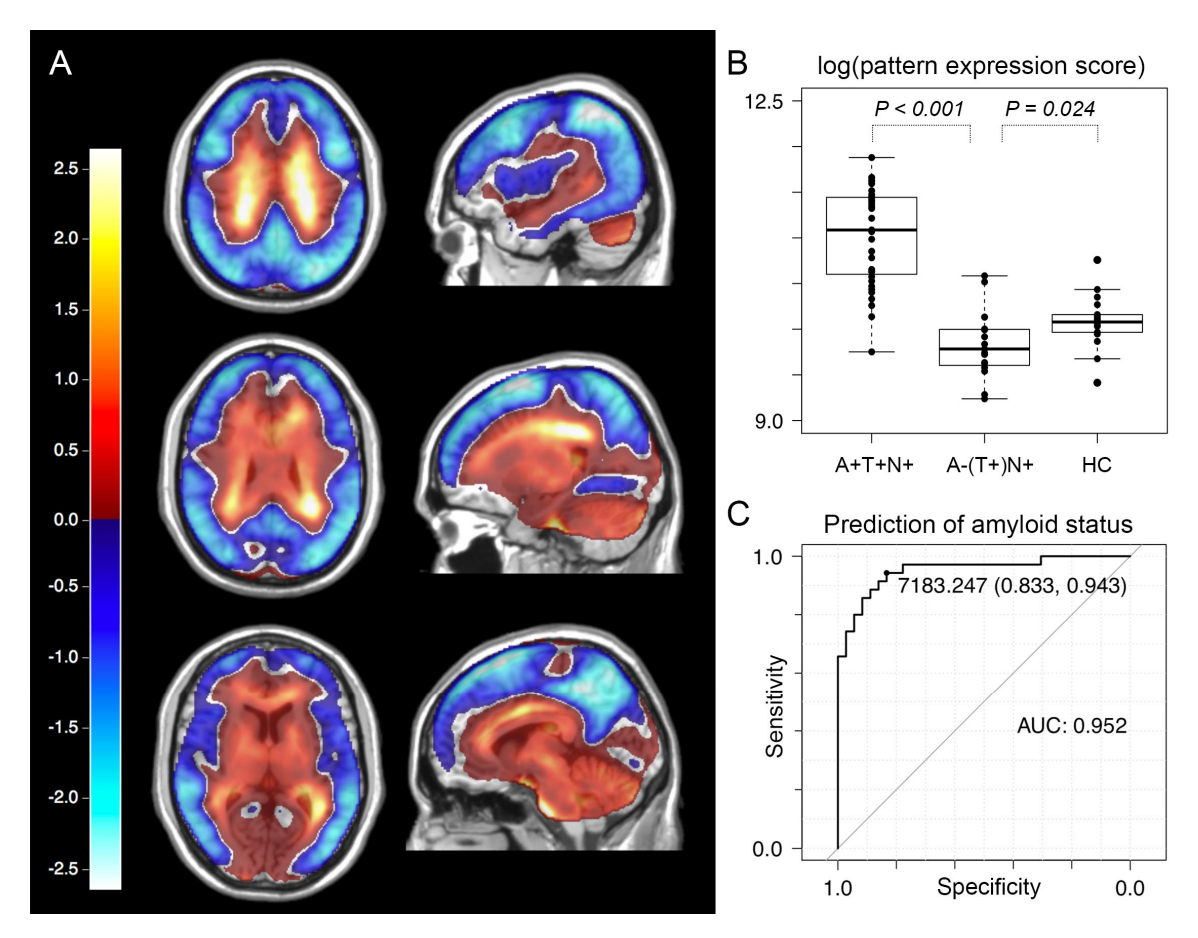


FIGURE 3: A) First component derived from SSM/PCA (explaining 29.5% of variance in the dataset) mainly consisting of positive values in the cerebral white matter and negative values predominantly in cortical areas that are typically affected in AD, i.e. precuneus, parietotemporal cortex and frontolateral cortex. B) Pattern expression scores of first SSM/PCA component in amyloid positive and negative patients as well as healthy controls (log-transformed for better visibility). C) ROC curve for prediction of amyloid status in all cases via pattern expression score of the first SSM/PCA component.

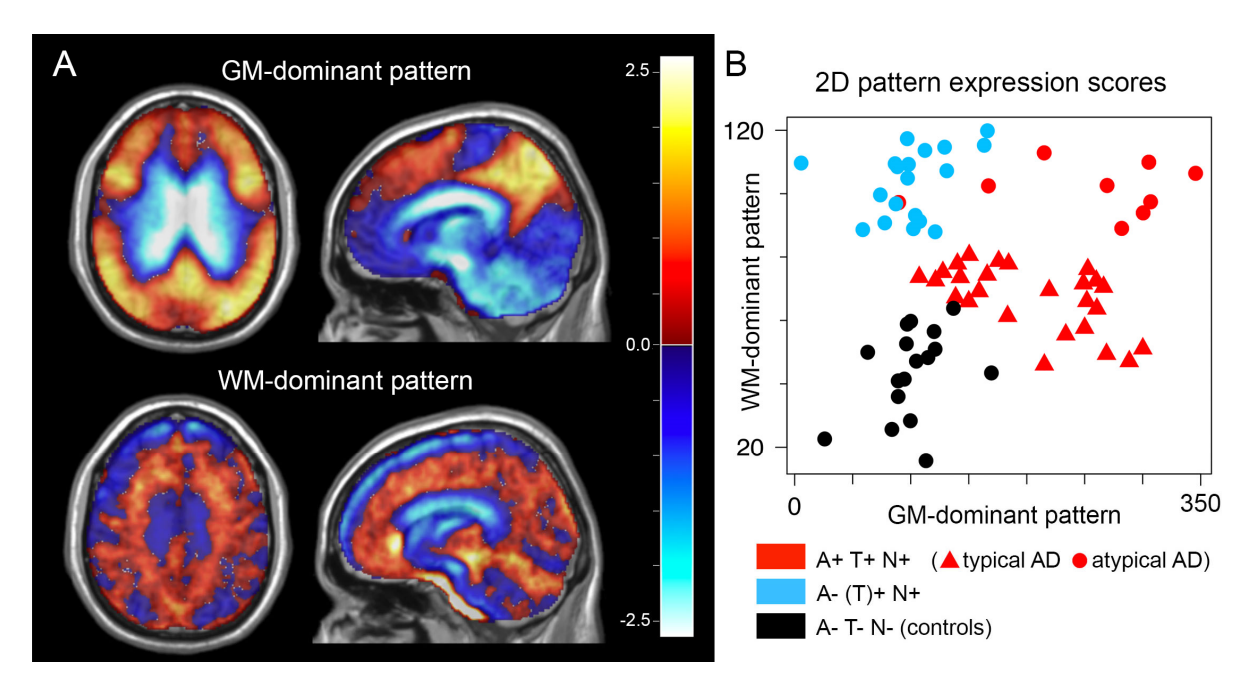
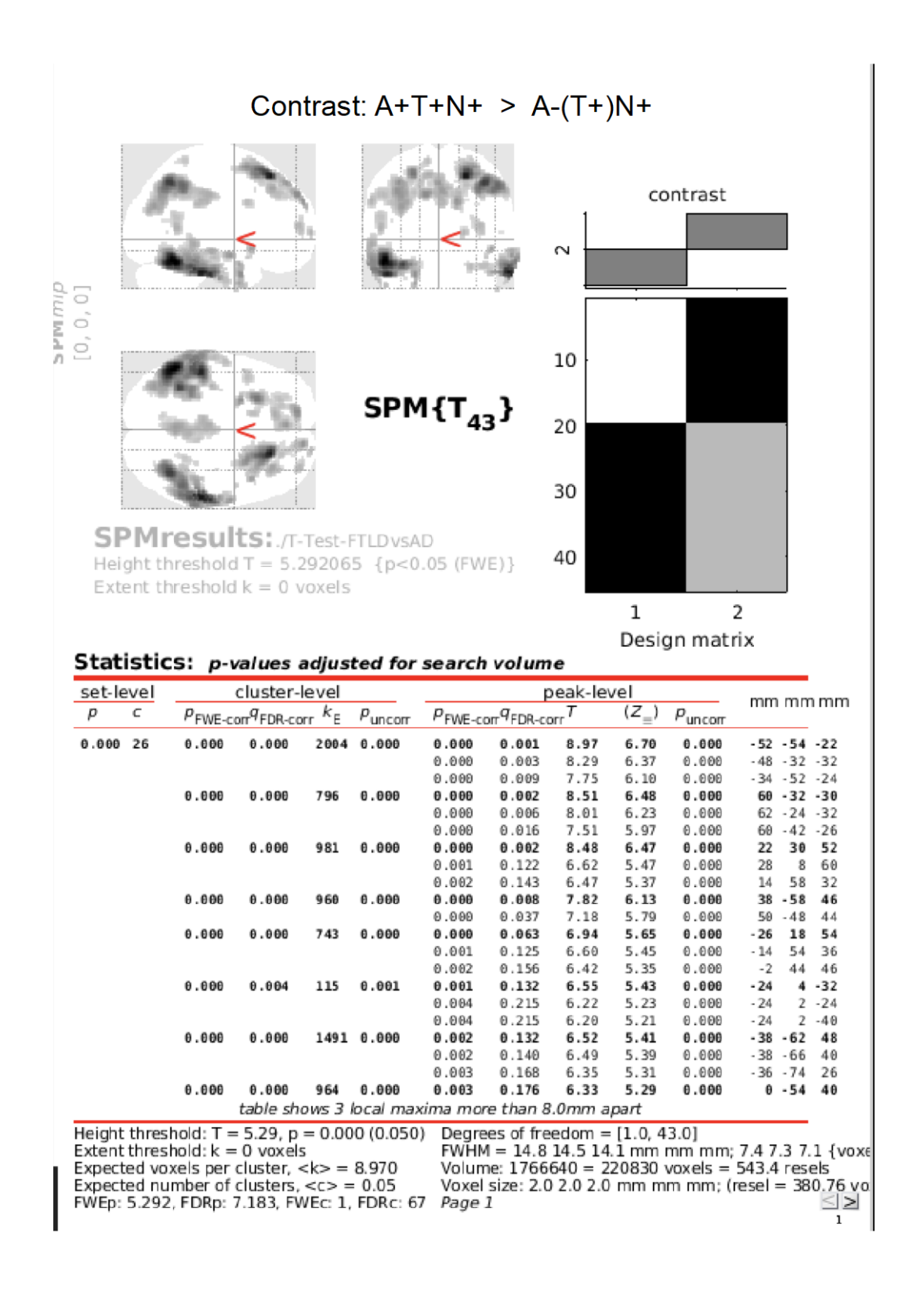


FIGURE 4: A) GM-dominant pattern derived from SSM/PCA of the subgroup containing A+T+N+ patients and healthy controls and WM-dominant pattern derived from SSM/PCA of a A-(T+)N+ patients controls B) 2-dimensional pattern expression scores used to predict amyloid status (square root transformed for better visibility). Interestingly, the expression of the WM-dominant pattern is higher in atypical AD cases, while it is relatively low in typical AD cases.

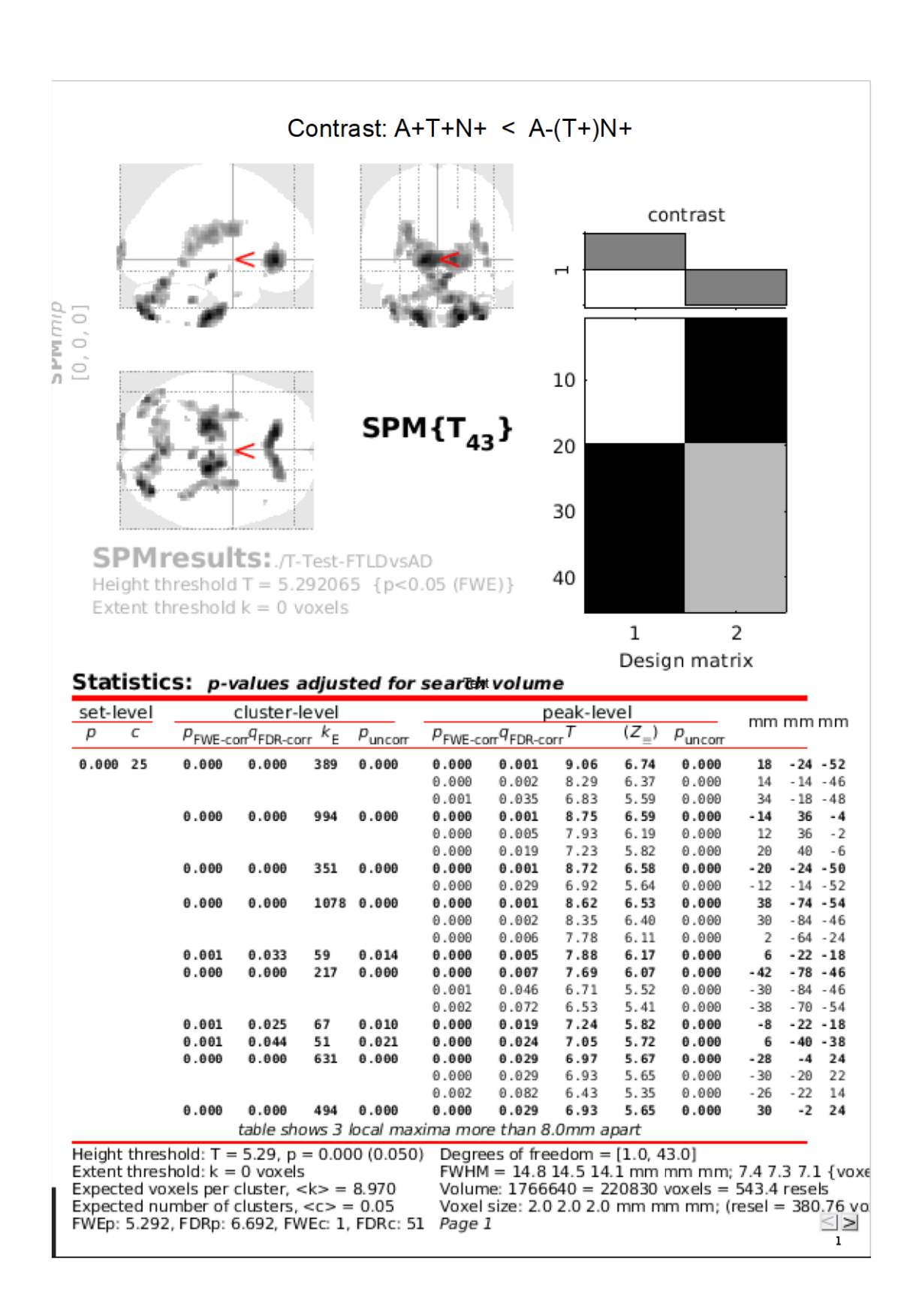
	A+T+N+	A-(T+)N+
n	35	19
Clinical diagnoses (n)	typical AD (26)	FTLD with aphasia (5)
	IvPPA (7)	bvFTD (11)
	bvAD (2)	FTLD-CBS overlap (1)
		FTLD with proven P301L
		mutation (1)
		FTLD-PSP overlap (1)
Average age in years	66.7 (7.1)	61.9 (11.3)
(standard deviation)		

Table 1: Patient characteristics (AD: Alzheimer's disease, FTLD: frontotemporal lobar degeneration, CBS: corticobasal-syndrome, PSP: progressive supranuclear palsy, lvPPA: logopenic variant of primary progressive aphasia, bvFTD: behavioral variant of frontotemporal dementia, bvAD: behavioral variant of AD)

Supplemental Data



SUPPLEMENTAL FIGURE 1: Result of voxel wise T-test in SPM comparing A+T+N+ to A-(T+)N+. Contrast: A+T+N+ > A-(T+)N+



SUPPLEMENTAL FIGURE 2: Result of voxel wise T-test in SPM comparing A+T+N+ to A-(T+)N+.

Contrast: A+T+N+ < A-(T+)N+